

Analysis of the complex impedance data for β -PbF₂

A. K. JONSCHER*, J. -M. RÉAU

Laboratoire de Chimie du Solide du CNRS, Université de Bordeaux I, 33405 Talence, France

Previously published complex impedance plots for the ionic conductor β -PbF₂ show the familiar depressed circular arcs with an angle $0.7 \pi/2$ and an activation energy for the volume conductivity $W_v = 0.45$ eV. A detailed analysis of this behaviour in terms of the recently developed “non-Debye” model shows the real part of the relative dielectric permittivity to have a frequency dependence $\omega^{0.7-1}$, with a high frequency limit of 50 Hz and with only weak dependence on temperature. The low-frequency “spurs” on the impedance plots are shown to indicate an interfacial barrier at each electrode having a similar “non-Debye” frequency characteristic to the bulk but showing a strong temperature dependence with an activation energy equal to $W_v/2$. This suggests the presence of low Debye-screened barriers of about kT height, resulting from depletion and accumulation of ionic carriers at incompletely transmitting electrodes. There is no visible effect of inter-grain boundaries on the flow of direct current.

1. Introduction

The continuing interest in the applications of fast ion conductors demands an improved understanding of their fundamental properties, the most directly important of which is their electrical conductivity. One of the classic methods of study is the determination of the alternating current (a.c.) impedance of samples, usually prepared in the form of compacted pellets sintered at elevated temperatures. The conventional analysis of these data gives the temperature dependence of the “volume” conductivity and also a parameter which defines the departure of the actual impedance diagram from a perfect semicircle. In the present paper we are taking the original numerical data on β -PbF₂, originally published by Réau *et al.* [1] and are subjecting them to a further detailed analysis following the suggested interpretation in terms of a “non-Debye” model of dielectric response [2] which is developed in more detail in the accompanying paper [3]. The procedure consists in inverting the impedance data and deriving the dielectric permittivity of the “volume”

regions, as well as the parameters of the “barriers”. The dependence of these parameters on both temperature and frequency enables certain conclusions to be drawn regarding the nature of the conduction mechanisms in this material.

Fig. 1 shows the reproduction of the original data [1] and it is clearly seen that the division into “volume” and “barrier” regions is well established, leading to an equivalent circuit of the series – parallel type shown in the inset, where the shaded capacitor denotes the “non-Debye” capacitance defined by Jonscher [2, 3]:

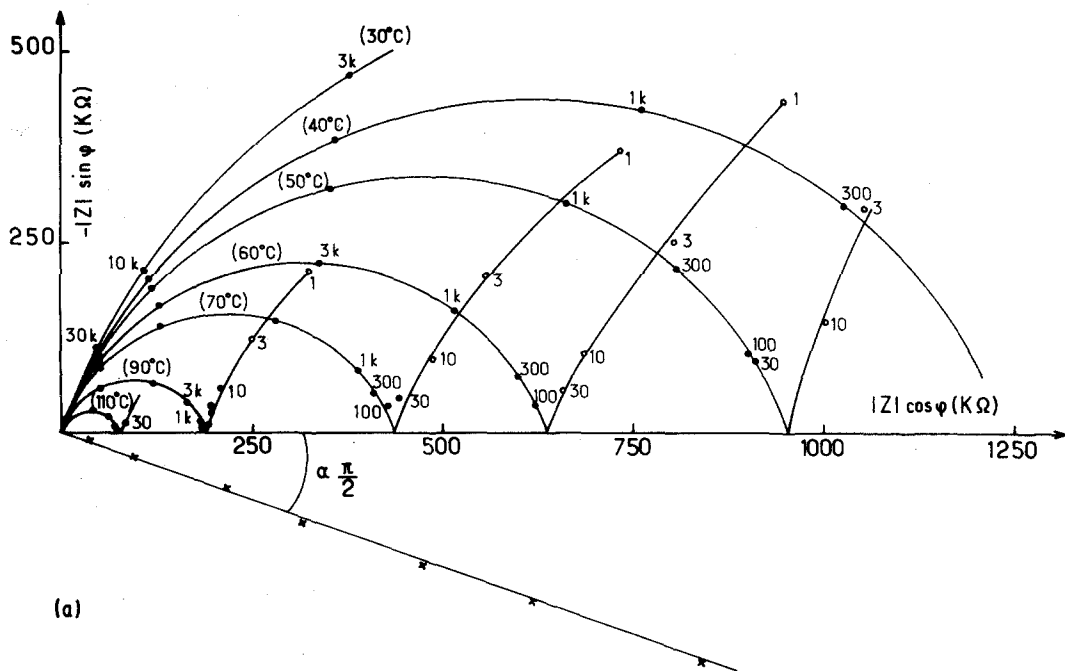
$$C_n(\omega) = B(i\omega)^{n-1}, \quad (1)$$

where B is a constant and the exponent n is less than unity. The angular frequency $\omega = 2\pi f$, where f is the circular frequency in Hertz, while $i = (-1)^{1/2}$.

2. “Volume” response

The high-frequency data correspond to well-developed inclined circular arcs passing through the origin of the Z -plane, within experimental

*Permanent address: Chelsea College, University of London, Pulton Place, London, UK.



(a)

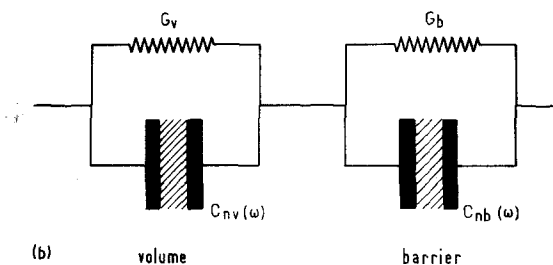


Figure 1 The complex impedance plot (a) for $\beta\text{-PbF}_2$ taken from the original reference by Réau *et al.* [1], (b) the equivalent circuit for the series combination of volume and barrier admittances, represented by the respective conductances G and “non-Debye” capacitors $C_n(\omega)$. (Numbers indicate frequencies in Hz.).

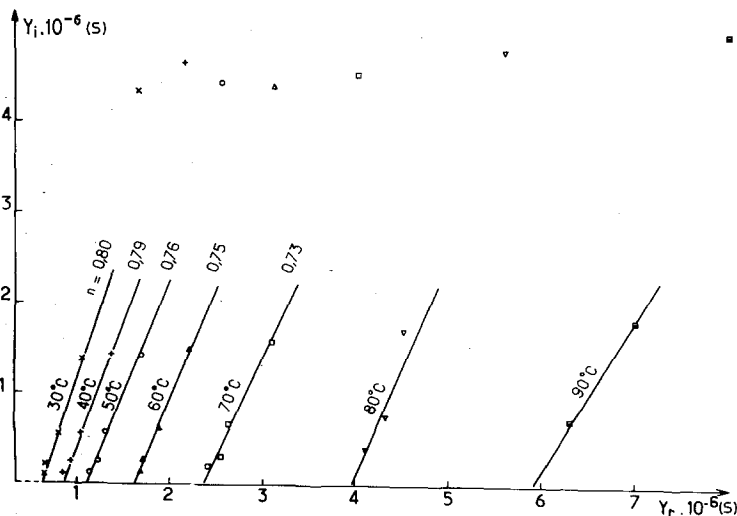


Figure 2 The complex admittance plots for the high-frequency parts of the circular arcs in Fig. 1. The straight lines are drawn through the lower frequency parts, the deviations at higher frequencies are explained in the text. The numerical values of the exponent n are determined from the slopes of these lines.

error, so that direct inversion into the admittance plane should give inclined straight lines. Fig. 2 shows the result of this operation for the lower temperatures. The data for the highest frequency clearly depart from the extrapolation of the straight lines which may be drawn through the lower-frequency points. This departure may be understood in terms of the onset of the high-frequency limit, ϵ_∞ , of the real part of the permittivity ϵ [2, 3]. The exponent n of the "non-Debye" capacitance $C_n(\omega)$ is seen to decrease steadily with rising temperature – a commonly observed trend – from $n = 0.80$ at 30°C to $n = 0.73$ at 60°C . At higher temperatures it is not possible to determine the value of n reliably since insufficient data points are available.

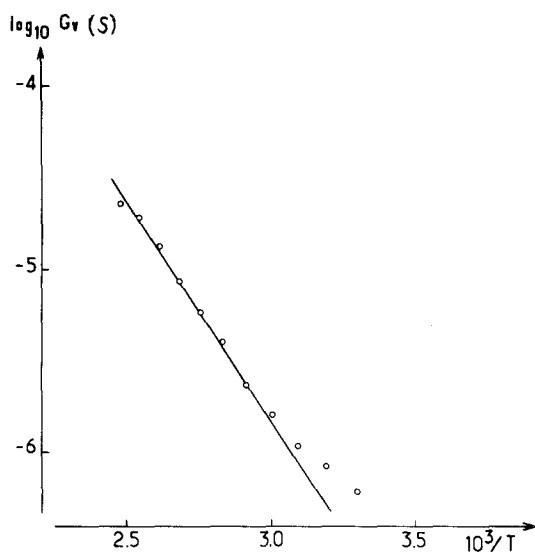


Figure 3 The volume d.c. conductance, G_v , plotted against the reciprocal temperature and showing an activation energy of 0.45 eV , with a tendency to a weaker temperature dependence at low temperatures.

The values of the parallel volume conductance, G_v , are plotted against the reciprocal temperature in Fig. 3 giving an activation energy $W_v = 0.45\text{ eV}$, in agreement with the original publication, except at lowest temperatures where a transition to a less strongly activated process is visible.

Using the values of the imaginary part of the complex admittance, Y_i , it is possible to derive the real part of the relative permittivity:

$$\epsilon'(\omega)/\epsilon_0 = Y_i/\omega C_0$$

where ϵ_0 is the permittivity of free space and C_0 is the geometrical capacitance of the sample taken to be 0.97 pF in the present instance. Fig. 4 shows the collected data for a range of temperatures over the frequency range 10 to 10^4 Hz . The manner of plotting these experimental points should be explained: in order to avoid a confusing density of points at the precise frequencies at which measurements were taken, points were displaced slightly along the trend of the curves so as to produce a clearer picture. A steady downward trend is clearly visible, more rapid at lower frequencies and tending to saturation at the upper end of the spectrum. The dispersion is stronger at higher temperatures, but data in the vital region become scarce because of the onset of the second stage "barrier" process.

The high-frequency data correspond to values of the relative permittivity in the range 50 to 70 , depending upon the temperature. While it is impossible to assert that this is exactly what one would expect of the high-frequency permittivity for this material, these values are sufficiently close to the probable value to be treated as corresponding to the bulk material and not to some "barrier" region in series with it. We consider this argument as justifying the treatment of the

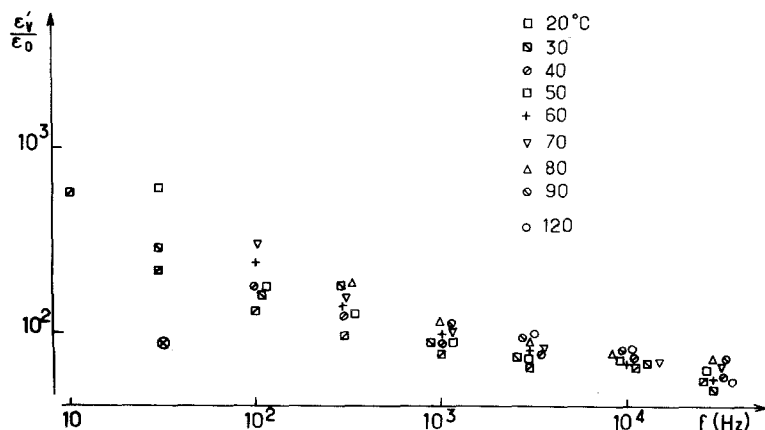


Figure 4 The real part of the relative dielectric permittivity, ϵ'_v/ϵ_0 for the volume response for the whole range of temperatures. The point A is a reference point for the normalization carried out in Fig. 5.

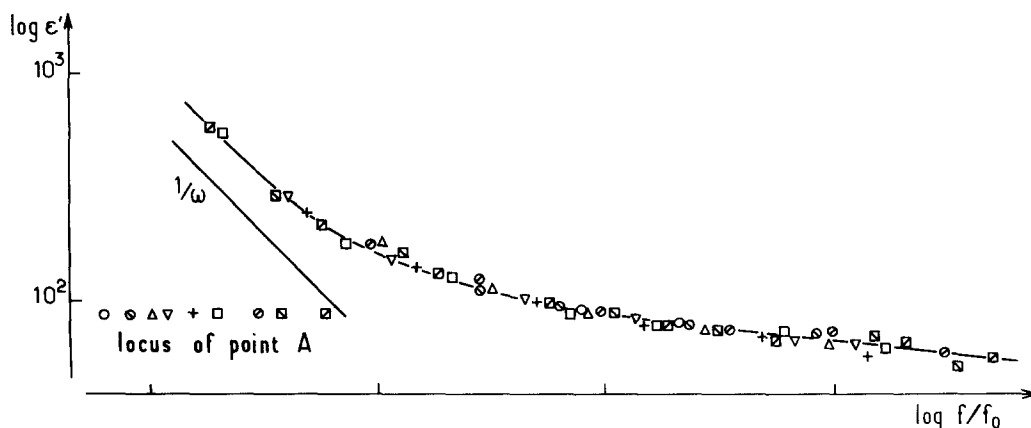


Figure 5 The data of Fig. 4 normalized by lateral displacement along the frequency axis to reveal a generalized frequency dependence. The locus of the point A in Fig. 4 is shown to give a measure of the displacements required.

principal circular arcs as representing true “volume” response of the material.

There is not much that one can do with these data with any certainty, but it is possible to achieve a greater clarity of results by invoking the well known fact, observed generally in many materials, that a variation of temperature has the effect of shifting the permittivity data along the frequency scale with only a slight change of the vertical scale. Bearing in mind the arbitrariness of this procedure, we apply it to the data of Fig. 4 and the result is shown in Fig. 5. The points appear to fall on a regular line which tends to a ω^{-1} dependence at lower frequencies and shows a slight slope at the higher end. It is not possible on the basis of the available data to discern a clear trend to saturation and no detailed comparison with the observed values of the slope n determined from the admittance graphs can be carried out reliably. The low-frequency behaviour is consistent with the observed trend in a wide range of materials with significant charge carrier densities contributing to polarization [3]. The symbols in the lower left-hand corner define the locus of the representative point “A” in Fig. 4, defining the shift of frequency with temperature. A plot of these data against $1/T$ gives an activation energy of 0.25 eV – within the limitations of the accuracy attainable in this procedure. This value is significantly lower than the d.c. activation energy, as is generally found to be the case.

It is unfortunate that the available data do not make it possible to plot meaningful graphs of the dielectric loss $\epsilon''(\omega)$, since this would require the determination of the values of G_0 with a much

higher precision than can be done from Fig. 2. Therefore the only source of information on the values of n is Fig. 2, no separate check is possible. However, the data of Fig. 5 may be considered to be compatible with the values of n so obtained if one bears in mind the $1/\omega$ trend at low frequencies and the existence of some high-frequency value ϵ_∞ at the upper end. We conclude that the bulk properties of the sample of $\beta\text{-PbF}_2$ show a definite “non-Debye” behaviour, with the values of n in the range 0.73 to 0.80 depending upon temperature and with a high-frequency value of ϵ_∞ of less than 50. The bulk d.c. conductivity has an activation energy of 0.45 eV, except at the lowest temperatures.

3. “Barrier” response

We now proceed to invert the low-frequency “spurs” of the impedance diagrams of Fig. 1 around the respective values of the d.c. volume conductance, forming the “barrier” admittances:

$$Y = (Z - 1/G_v)^{-1}. \quad (2)$$

The results of this operation are seen in Fig. 6 for the lower temperatures for which the frequency data are not very extended. It is immediately evident that these admittance plots represent effectively straight lines passing through the origin, indicating very low values of d.c. barrier conductances – the barriers appear as just “non-Debye” capacitances. The values of the exponent n for the barrier found from the slopes of these lines fall in the range around 0.6. The slight variations for the different temperatures cannot be considered to be significant.

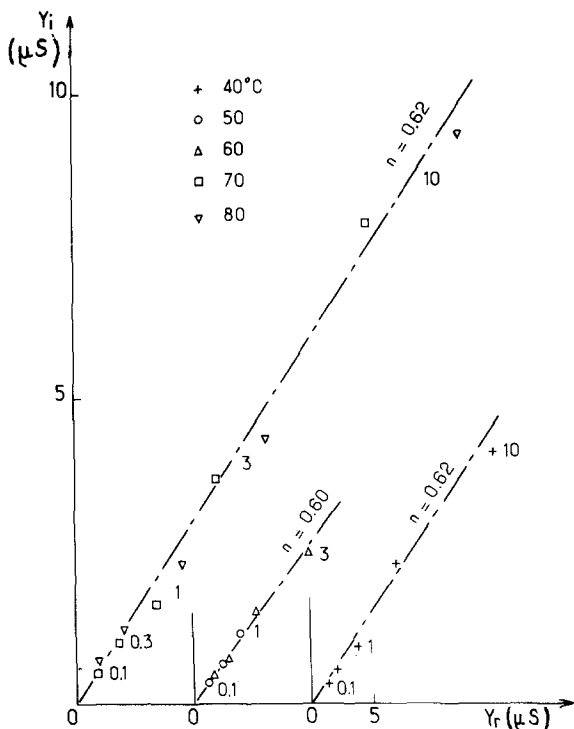


Figure 6 The complex admittance plots of the lower-frequency parts of the "spurs" in Fig. 1, for the five lowest temperatures for which the data are available. The respective sets of points are displaced laterally for clarity and all lines are going through the origin. The figures indicate frequencies in Hz.

The high temperature data for 110, 120 and 130°C offer a wider scope in view of the wider range of frequencies and they also present a somewhat different picture. The intercept G_b corresponding to the barrier conductance under d.c. conditions is now measurable and has the following values:

$$110^\circ \text{C} \quad G_b = 0.26 \mu\text{S}$$

$$120^\circ \text{C} \quad G_b = 0.6 \mu\text{S}$$

$$130^\circ \text{C} \quad G_b = 1.5 \mu\text{S}$$

With these values it is now possible to plot the logarithmic admittance diagram, $\log(Y_r - G_b)$ versus $\log Y_i$ which enables a better assessment of the extent of agreement to be obtained than in the linear representation [4]. The results are shown in Fig. 7. The highest temperature data show the best fit with a value of $n \approx 0.73$, the 120°C data follow a similar trend with a slightly lower value of n and finally the 110°C points give a rather poor fit, with a tendency to much lower values of n . What is surprising in these data are the relatively

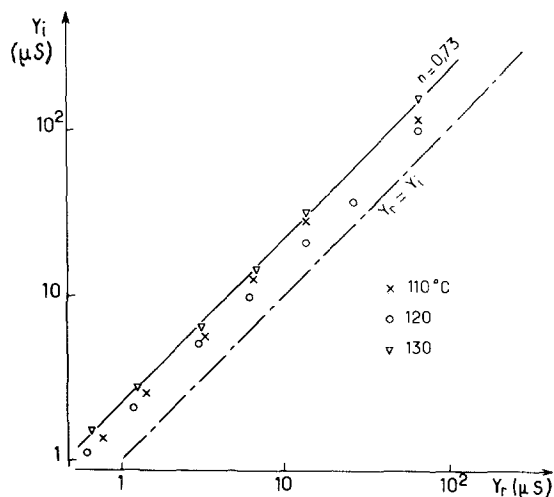


Figure 7 The logarithmic complex admittance the low-frequency data at the three highest temperatures. The chain-dotted line corresponds to $Y_r = Y_i$, the vertical displacement from this line gives the slope of the linear admittance plot.

higher values of n than at the lower temperatures – somewhat contrary to the trend observed generally. It may be that the lower-temperature data are to be treated with some reserve, bearing in mind the relatively restricted ranges of frequency involved. The values of n obtained from the high-temperature barrier data are in reasonably close agreement with those corresponding to the bulk material.

We are now able to investigate the behaviour of the barrier capacitance both as function of temperature and of frequency. Fig. 8 shows the frequency dependence of G_b at ten different temperatures in the frequency range 0.1 to 100 Hz, giving a typical "non-Debye" behaviour with n in the range 0.6 to 0.7, allowing for some scatter of the experimental points. No saturation at high frequencies is apparent. The capacitance is seen to increase with rising temperature, the increase being of the order of a factor of ten between 20 and 130°C.

In order to investigate the temperature dependence of capacitance in more detail we take the data at 0.1 Hz as representative of the behaviour throughout the frequency range while being the most reliable. Fig. 9 shows that C_b has a simple activation energy of 0.20 eV with a very good fit to the exponential dependence on $1/T$. We note the very high values of C_b relative to C_v corresponding to a ratio of 6×10^3 at the

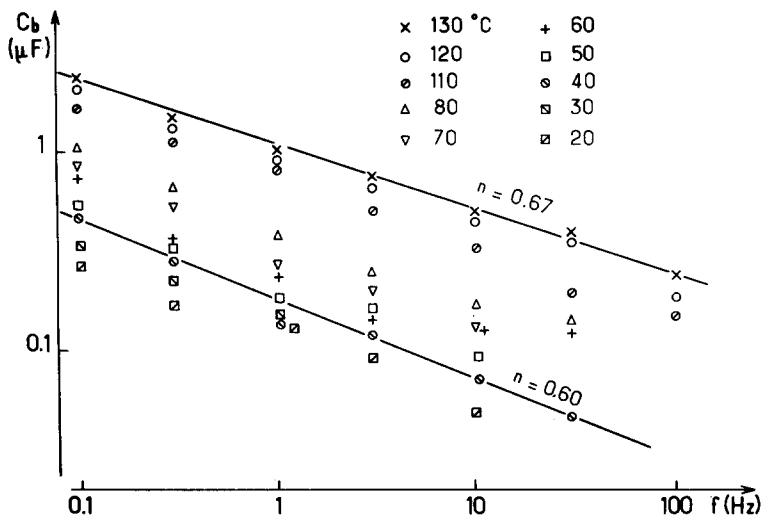


Figure 8 The frequency dependence of the barrier capacitance with the temperature as the parameter.

lower temperatures and 3×10^4 at the higher. The only reasonable interpretation of this is that barrier represents a correspondingly small part of the total thickness of the sample. We may write the following relation:

$$\frac{C_b}{C_v} = \frac{\epsilon_b w_v}{\epsilon_v w_b} \approx \frac{w_v}{w_b} \quad (3)$$

where the w 's denote the thicknesses of the respective regions and the last approximate equality

is based on the assumption that $\epsilon_b \approx \epsilon_v$, which appears to be very reasonable on physical grounds. Given the sample thickness $w_v = 1.2$ mm, we may obtain the thickness of the barrier-

$$w_b = w_v C_v / C_b \quad (4)$$

taking for C_v the temperature-dependent values at the high-frequency end of the spectrum in Fig. 5, as most likely to correspond to the "intrinsic" properties of the bulk material. The resulting temperature dependence of the barrier thickness is shown in Fig. 9 with an activation energy of 0.17 eV. The sense of the dependence — the thickness decreasing with rising temperature — seems to rule out any form of "chemical" barrier due to some interfacial chemical changes.

A thermally activated capacitance is most likely due to some transport processes in the neighbourhood of the barrier and we may rule out injection of excess carriers from the electrodes as not giving sufficiently large capacitive effects [4], while the opposite phenomenon of a Schottky barrier at the interface would not lead to a thermally activated barrier width. This leaves the third possibility; a small-signal capacitance arising from a near-equilibrium situation near an incompletely replenishing electrode, where the interfacial field is screened within a Debye length λ and the resulting capacitance per unit area is given by the expression:

$$C_b = \epsilon_v / \lambda = [e^2 \epsilon_v N / kT]^{1/2} \quad (5)$$

where e is the magnitude of the electronic charge and N is the density of mobile ions. This density is clearly thermally activated and apart from the

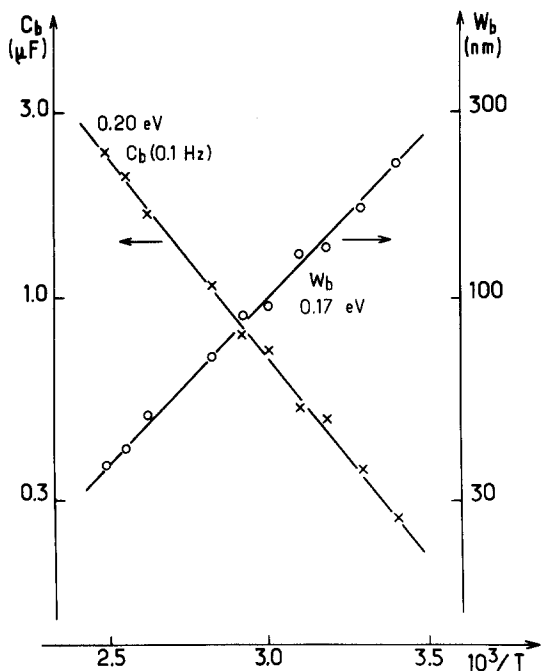


Figure 9 The logarithmic plot of the barrier capacitance, C_b , and the corresponding barrier width w_b , versus reciprocal temperature, showing the activation energies.

factor T , is the only significantly temperature-dependent parameter. This shows that C_b has approximately half the activation energy of the volume charge density N .

With regard to the expected orders of magnitude, we note that N must be of the form:

$$N = N_0 \exp(-W_v/kT) \quad (6)$$

where N_0 is the total density of the available ionic carriers, while the activation energy W_v represents the appropriate magnitude for carrier numbers, which will be assumed to be equal to or very slightly smaller than the conductivity activation energy [5] from Fig. 3. N_0 will be taken as the number of F^- ions, which is of the order 10^{28} m^{-3} . Taking ϵ_v as found in Fig. 4 at high frequencies, we note that the values of w_b in Fig. 9 are reproduced within a factor of 2 or 3 which represents an excellent agreement. This interpretation does not at present explain the fact that the barrier capacitance shows a slightly strongly frequency dependence, proportional to ω^{n-1} with $n = 0.6$ to 0.7 , in comparison with the volume permittivity for which $n = 0.7$ to 0.8 .

The important further conclusion is that we do not require more than just two barriers, one at each electrode, despite the polycrystalline nature of our sample. Moreover, this barrier is not the Schottky type, with a large potential barrier for carrier flow, but its height is measured in millivolts, $\sim kT$ or so, and it arises solely from incomplete replenishment at the electrode. It is interesting to note that with the relatively high densities of mobile carriers involved there is little chance of a barrier of significant height to be developed – the interfacial charge densities involved would be prohibitively high.

We may now look in more detail at the effective parallel conductance of the barrier, G_b . The temperature dependence is shown in Fig. 10a which indicates an activation energy of 1.2 eV , albeit over a very restricted temperature range. There can be no doubt of a much more rapid temperature dependence of G_b in comparison with the volume conductance G_v . It is interesting to attempt to deduce the conductivity of the barrier region, by multiplying by the appropriate barrier thickness, derived from Fig. 9. In this way we obtain Fig. 10b, which suggests an activation energy for conductivity of 0.95 eV , with the absolute level of conductivity of the order $10^{-10} \text{ S m}^{-1}$.

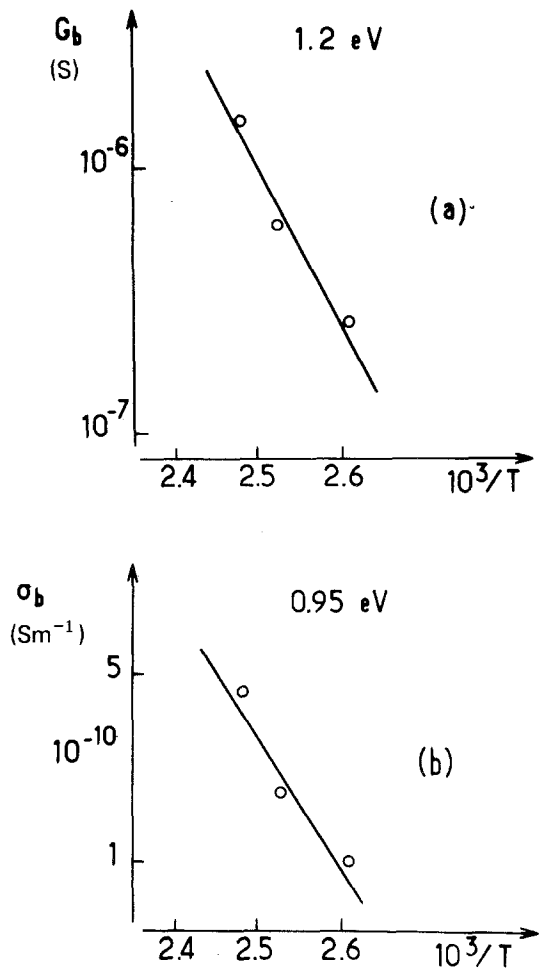


Figure 10 The activation energy of the barrier conductance G_b , (a) and of the corresponding conductivity σ_b (b).

4. Conclusions

Our analysis of the complex impedance behaviour of $\beta\text{-PbF}_2$ has revealed a number of features which are not normally appreciated in the conventional approach. The bulk behaviour is seen very clearly to consist of the superposition of a strongly temperature-dependent volume d.c. conductance with an activation energy 0.45 eV , and of a weakly temperature-dependent “non-Debye” admittance with exponent $n = 0.7$ and a frequency activation energy 0.24 eV .

The analysis of the barrier behaviour reveals hitherto unappreciated results. Firstly, the barrier is seen to consist of a “non-Debye” admittance having a similar characteristic value of n to the bulk. The absolute value of the capacitance indicates a thin region, between 30 and 300 nm in thickness, with a clear activation energy of

slightly less than half the bulk conductivity activation energy. This points clearly to a "Debye-Hueckel" type screening capacitance, of a very small barrier height and arising from local depletions and accumulations of charge carriers at an incompletely replenishing electrode. Superimposed upon this barrier capacitance is a barrier conductance with an activation energy of approximately 1 eV. This must be due to the motion of some other ionic species which becomes dominant once the normal densities have become depleted.

We are therefore led to the following model of the electrical properties of β -PbF₂. The material consist of a "lattice" or "matrix" which has a characteristic "non-Debye" behaviour and which normally contains a high density of mobile ionic carriers capable of giving d.c. conduction with an activation energy of 0.45 eV. The high mobility or low activation energy of these carriers arises from the existence of a large surplus of potentially vacant sites among which they may hop.

Any local depletion or accumulation of these charges resulting from an incompletely replenishing electrode gives rise to a capacitance, whose temperature dependence is dictated by the bulk activation energy while the frequency dependence is just that of the bulk matrix.

The "non-Debye" response of this matrix may be interpreted in one of three principal ways. One of these may be described as the "distribution of relaxation times" school and it is too vague to be commented on in detail – it simply postulates that the inclined circular arcs are the result of some distribution of parameters in the material. We have already criticised this approach elsewhere [2, 3] and will leave the matter at that. The alternative accepted approach is that of Macdonald [6] who seeks to explain the entire complex impedance behaviour in terms of interfacial phenomena limiting the transmission of charge carriers, i.e. in terms of effective capacitive-resistive series networks. In order to explain the inclined circular arcs this model has effectively to postulate some form of distribution of barrier parameters, rather like the former model, but admittedly on a physically more specific basis. On the basis of the limited amount of data at our

disposal we are unable to refute or to confirm this model at the present stage. However, Macdonald's model would have to be applied to the interpretation of the observed temperature dependence of the barrier capacitance and, in particular, to the similarity between the frequency dependence of the barrier and of the bulk permittivity. While reserving judgement on this point, we are led to the third alternative, the model postulated by one of us [2, 3] and based on the concept of "screened" hopping conduction [7].

This model should be eminently applicable to fast ion conductors since the carriers in them necessarily move by hopping between preferred localized sites. There is also no doubt about the presence of mutual interactions resulting in screening, in view of the large densities of the charges involved, and this is in qualitative agreement with a recent model derived by Wang *et al* [8] who had to postulate simultaneous cooperative movements of several Na⁺ ions in β -alumina. Although the present discussion relates specifically to β -PbF₂, we have evidence that similar behaviour is seen in other ionic conductors, so the proposed model is likely to have more general significance.

Acknowledgements

One of us (AKJ) is grateful to Professor P. Hagemuller for his hospitality during the tenure of a Visiting Professorship in his Laboratory.

References

1. J. -M. RÉAU, J. CLAVERIE, G. CAMPET, C. DEPORTES, D. RAVAINÉ, J. -L. SOUQUET and A. HAMMOU, *C. R. Acad. Sci. (Paris)* **280** (1975) 325.
2. A. K. JONSCHER, *Phys Stat. Solidi* (a) **32** (1975) 665.
3. *Idem*, *J. Mater. Sci.*, **13** (1978) 553.
4. *Idem*, *Thin Solid Films*, **36** (1976) 1.
5. A. K. JONSCHER and R. M. HILL, "Physics of Thin Films", edited by M. H. Francombe, Vol. 8 (Academic Press, 1975) p. 169.
6. J. ROSS MACDONALD, "Electrode Processes in Solid State Ionics", edited by M. Kleitz and J. Dupuy, (D. Reider, Dordrecht 1976) p. 149.
7. A. K. JONSCHER, *Nature* **253** (1975) 717.
8. J. C. WANG, M. GAFFARI and SANG-IL CHOI, *J. Chemical Phys.* **63** (1975) 772.

Received 12 May and accepted 17 June 1977.